Hydroelastic Vibration of Free-Edge Annular Plates

M. K. Kwak

Department of Mechanical Engineering,
Dongguk University,
26 Pil-Dong 3-Ga, Joong-Gu,
Seoul 100-715, KOREA

M. Amabili

Department of Industrial Engineering,
University of Parma,
Parma 43100, Italy

This paper is concerned with the virtual mass effect due to the presence of water on the natural frequencies of free-edge annular plates resting on free surface or completely submerged, which has never been studied theoretically. Experiments were carried out for free-edge annular plates to find the so-called nondimensionalized added virtual mass incremental factors. In this paper, theoretical nondimensional added virtual mass incremental factors are obtained by employing the Hankel transformation technique in conjunction with the Fourier-Bessel series approach. It is found that the theoretical nondimensionalized added virtual mass incremental factors for free-edge annular plates resting on free-surface agree well with experimental ones. The proposed method can be applied to different boundary conditions of plates.

1 Introduction

It is generally known that the natural frequencies of structures which are in contact with water, or immersed in water, decrease significantly compared to the natural frequencies in air. This is due to the fact that the vibration of a structure in contact with water is transferred to the water motion and results in a discernible increase in the kinetic energy of the total system. This problem is referred to as the fluid-structure interaction problem. The first fluid-structure interaction problem stems from the classical problems solved by Lord Rayleigh (1877) and Lamb (1921). They investigated the increase of inertia due to the presence of water and suggested the use of the approximate formula based on the so-called added virtual mass incremental (AVMI) factor, which is the ratio between the kinetic energy of the water and the kinetic energy of the structure. Lamb (1921) calculated the change in the natural frequencies of a thin circular plate clamped along its boundary and placed in the aperture of an infinite rigid plane baffle in contact with water.

Lamb's work initiated the study on the vibration of circular plates in contact with water. Since his study, there have been numerous theoretical and experimental investigations on vibration of circular plates in contact with water (Powell and Roberts, 1923; McLachlan, 1932; Peake and Thurston, 1954; Espinosa and Gallego-Juarez, 1984; Kwak and Kim, 1991; Kwak, 1991, 1996; Amabili et al., 1995). It is worthwhile to be noted here that the problem solved by Kwak and Kim (1991) and Kwak (1991) is different from the Lamb's original problem since they considered the case of circular plates resting on free surface. The kinetic energy increases when the rigid-wall condition is imposed instead of free-surface condition since the rigid wall constrains the motion of water at the interface. They found that the nondimensionalized added virtual mass incremental (NAVMI) factors for the simply-supported and clamped circular plates are considerable lower than those obtained by Lamb (1921) and Peake and Thurston (1954) but the NAVMI factors for the free-edge circular plate are almost identical in both cases.

The advantage of using NAVMI factors is that the characteristics of the fluid-structure interaction problem can be understood qualitatively and they are easy to use. However, the NAVMI factors are available only for the circular plates and rectangular plates in simple fluid domains. If someone wishes to solve a fluid-structure interaction problem which involves complex geometry of a structure and water domain, he should resort to the finite element modeling of fluid (FFEM) or the boundary element method (BEM) in conjunction with finite element modeling of structures. However, the use of the FFEM or the BEM requires amounts of time on modeling and computation. In addition, it is quite difficult to obtain the qualitative measure of water effect by those methods.

In this paper, the NAVMI factors for a uniform free-edge annular plate vibrating in free surface are obtained. A similar problem was solved by Amabili et al. (1996), and Amabili (1996) but the annular plate is assumed to be placed into a hole of the rigid wall in their works. Hence, the boundary condition considered in this paper is different from the one considered in the previous papers (Amabili et al., 1996; Amabili, 1996). The boundary value problem for the annular plate resting on free surface results in a triply mixed boundary value problem due to its boundary conditions. Notice that the triply mixed boundary value problem has never been addressed in the previous papers. Here we consider the case experimentally studied by Amabili (1994). To solve the triply mixed boundary value problem and verify the experimental results, the Fourier-Bessel series approach used by Tranton (1950, 1954) is employed, which proved to be effective for the vibration problem of circular membranes and circular plates in contact with water (Kwak, 1994, 1996).

In the theoretical analysis, we assume that the "wet" modes are almost identical with the "dry" modes. Experimentally it has been verified by Espinosa and Gallegro-Juarez (1986) and more specifically by Amabili et al. (1995) that mode shapes of free-edge circular plates immersed in water are very close to ones of plates in air. This assumption plays a very important role in this problem; we can decouple the fluid-structure interaction problem and derive a simple formula for the addressed problem. In fact, this amounts to saying that we can use the eigenfunctions of the annular plate vibrating in air to solve the hydroelastic problem of the annular plate immersed in water. We also assume that fluid is inviscid and imcompressible, and the thickness of the plate is thin relative to its radius; fluid sloshing at the free surface is neglected.

In order to verify the theoretical results, experiments were carried out. It is found from the results that the theoretical NAVMI factors agree well with the experimental ones, thus validating the approach developed in this paper.

Copyright © 1999 by ASME

2 Added Virtual Mass Incremental Factor

Let us consider an annular plate resting on free water surface, which has an outer radius, a, an inner radius, b and thickness, h. As mentioned above, we will use the assumption that the wet mode shapes are the same as the dry mode shapes. This assumption plays a very important role in solving the fluid-structure interaction problem and enables us to separate the coupled problem into two independent boundary value problems as will be seen.

The Rayleigh quotient can be applied to higher modes if the admissible functions are the exact eigenfunctions of the given problem. Based on the assumption, we can extend the theory to the higher wet modes. Thus, we can write the Rayleigh quotients for dry and wet cases as follows:

$$f_a = \frac{1}{2\pi}\sqrt{\frac{V_p}{T_p^*}}, \quad f_w = \frac{1}{2\pi}\sqrt{\frac{V_p}{T_p^* + T_w^*}} \qquad (1)$$

where f_a is the natural frequency of plates in air, f_w is the natural frequency of plates in contact with water, T_p^* and V_p represent the reference kinetic energy and the maximum potential energy of the circular plate, respectively, and T_w^* represents the reference kinetic energy of water due to the motion of the circular plate. The relation between the reference and maximum kinetic energy can be written as $T_{\max} = T^*\omega^2$ (Meirovitch, 1986), where ω is the circular frequency in radians per second.

Hence, the natural frequency in water can be expressed in terms of the natural frequency in air

$$f_w = \frac{f_a}{\sqrt{1+\gamma}}, \qquad (2)$$

where γ represents the added virtual mass incremental (AVMI) factor defined by the ratio of the kinetic energy of water due to the motion of the circular plate over the kinetic energy of the circular plate itself, i.e.,

$$\gamma = \frac{T_w^*}{T_p^*} = \Gamma\left(\frac{\rho_w a}{\rho_p h}\right) = \Gamma\beta \qquad (3)$$

where ρ_w is the density of water, ρ_p is the mass density of the circular plate and Γ is the nondimensionalized added virtual mass incremental (NAVMI) factor which is a function of mode shapes and boundary conditions, and $\beta = \rho_w a/\rho_p h$, is called a thickness correction factor, respectively. The objective of this paper is to compute Γ.

The differential equation of motion for the annular plate vibrating in vacuo can be written as

$$D_E \nabla^4 w(r, \theta, t) + \rho_p \frac{\partial^2 w(r, \theta, t)}{\partial t^2} = 0 \qquad (4)$$

where $w(r, \theta, t)$ is the deflection of the plate, $D_E = Eh^3/12(1-\nu^2)$ is flexural rigidity, E is Young's modulus and ν is Poisson's ratio, respectively. By separation of variables and assuming harmonic motion, the solution of Eq. (4) is expressed as;

$$w(r, \theta, t) = \sum_{s=0}^{\infty}\sum_{n=0}^{\infty} W_{sn}(r) \cos s\theta \sin \omega t \qquad (5)$$

where ω is a function of the dimensionless parameter λ_{sn} and

$$W_{sn}(r) = A_{sn} J_s\left(\frac{\lambda_{sn} r}{a}\right) + B_{sn} Y_s\left(\frac{\lambda_{sn} r}{a}\right)$$

$$+ C_{sn} I_s\left(\frac{\lambda_{sn} r}{a}\right) + D_{sn} K_s\left(\frac{\lambda_{sn} r}{a}\right) \qquad (6)$$

represents the eigenvector corresponding to specified nodal diameter and nodal circle in which J_s, Y_s, I_s and K_s are the Bessel function of the first kind and second kind, and the modified Bessel function of the first kind and second kind of order s, respectively. λ_{sn} (the eigenvalues), A_{sn}, B_{sn}, C_{sn} and D_{sn} are determined by applying the boundary conditions. The values of these coefficients for free-edge annular plates are given by Vogel and Skinner (1965) but are re-evaluated for the present study.

Next we consider the water domain which the plate is contact with. The three-dimensional oscillatory flow in cylindrical coordinates can be described by the velocity potential

$$\Phi(r, \theta, z, t) = \phi(r, z) \cos s\theta \, \omega \cos \omega t \qquad (7)$$

where the spatial velocity potential, $\Phi(r, \theta, z, t)$, satisfies the Laplace equation, $\nabla^2\Phi(r, \theta, z, t) = 0$. Considering the plate to be impermeable, the velocities of water and the plate particle in contact are identical at the water-plate interface. Also, the velocity potential becomes zero at free-surface if we assume that frequency is large (neglecting sloshing). In addition, the radiation condition requires that the disturbance attenuates as the distance from the plate becomes large. Hence, the boundary value problem for an annular plate vibrating in contact with water can be written as

$$\frac{\partial^2\phi}{\partial r^2} + \frac{\partial\phi}{r\partial r} + \frac{\partial^2\phi}{\partial z^2} - \frac{s^2}{r^2}\phi = 0 \qquad (8)$$

$$\left.\frac{\partial\phi}{\partial z}\right|_{z=0} = -W_{sn}(r) \quad b < r < a \qquad (9)$$

$$\phi(r) = 0 \quad 0 < r < b, r > a \qquad (10)$$

$$\phi, \frac{\partial\phi}{\partial r}, \frac{\partial\phi}{\partial z} \to 0 \quad \text{as} \quad r, z \to \infty \qquad (11)$$

The boundary value problem consisting of partial differential Eq. (8) and boundary conditions (9), (10) and (11) is conveniently handled by means of an integral transform. Considering the cylindrical coordinate system (r, θ, z), the obvious choice is the Hankel transformation (Sneddon, 1951), which is denoted by

$$\bar{\phi}_h(\xi, z) = \int_0^\infty r\phi(r, z) J_s(\xi r) dr \qquad (12)$$

Moreover, we can derive the following relation by integrating by parts,

$$\int_0^\infty r\left(\frac{\partial^2\phi}{\partial r^2} + \frac{\partial\phi}{r\partial r} - \frac{s^2}{r^2}\phi\right) J_s(\xi r) dr = -\xi^2\bar{\phi}_h(\xi, z) \qquad (13)$$

Multiplying Eq. (8) by $rJ_s(\xi r)dr$, integrating over the entire radius, and using Eqs. (12) and (13), the partial differential equation, Eq. (8), is reduced to the ordinary differential equation,

$$\frac{d^2\bar{\phi}_h}{dz^2} - \xi^2\bar{\phi}_h = 0 \qquad (14)$$

From the boundary condition (11), we conclude that the solution of Eq. (14) should consist of the attenuating part only. Therefore, the solution of Eq. (14) has the form of

$$\bar{\phi}_h(\xi, z) = B(\xi)e^{-\xi z} \qquad (15)$$

Using the inversion formula of the Hankel transformation and Eq. (15), we obtain

$$\phi(r, z) = \int_0^\infty \xi \bar{\phi}_h(\xi, z) J_s(\xi r) d\xi$$

$$= \int_0^\infty \xi B(\xi) e^{-\xi z} J_s(\xi r) d\xi \qquad (16)$$

Inserting Eq. (16) into the boundary conditions (9) and (10) yields

$$\int_0^\infty \xi^2 B(\xi) J_s(\xi r) d\xi = -W_{sn} \quad b < r < a \qquad (17)$$

$$\int_0^\infty \xi B(\xi) J_s(\xi r) d\xi = 0 \quad 0 < r < b, r > a \qquad (18)$$

We can nondimensionalize our variables by introducing new variables

$$\sum_{m=0}^\infty a_m \int_0^\infty J_{s+2m+2}(\eta) J_s(\rho\eta) d\eta$$

$$+ \sum_{l=0}^\infty b_l \int_0^\infty J_{s+2l+2}(\delta\eta) J_s(\rho\eta) d\eta$$

$$= -F_{sn}(\rho) \quad \text{for} \quad \delta < \rho < 1 \qquad (24)$$

$$\sum_{m=0}^\infty a_m \int_0^\infty \eta^{-1} J_{s+2m+2}(\eta) J_s(\rho\eta) d\eta$$

$$+ \sum_{l=0}^\infty b_l \int_0^\infty \eta^{-1} J_{s+2l+2}(\delta\eta) J_s(\rho\eta) d\eta$$

$$= 0 \quad \text{for} \quad 0 < \rho < \delta \qquad (25)$$

If we evaluate integrals using the mathematical table [Gradshteyn and Ryzhik, 1994; Eqs. (6.512) and (6.574)], then we obtain

$$\sum_{m=0}^\infty a_m \frac{\rho^s \Gamma(\frac{3}{2} + m + s)}{\Gamma(\frac{3}{2} + m)\Gamma(1 + s)} \,{}_2F_1\left(\frac{3}{2} + m + s, -\frac{1}{2} - m, 1 + s, \rho^2\right)$$

$$+ \sum_{l=0}^\infty b_l \frac{\delta^{2+2l+s}\Gamma(\frac{3}{2} + l + s)}{\rho^{3+2l+s}\Gamma(-\frac{1}{2} - l)\Gamma(3 + 2l + s)} \,{}_2F_1\left(\frac{3}{2} + l + s, \frac{3}{2} + l, 3 + 2l + s, \frac{\delta^2}{\rho^2}\right) = -F_{sn}(\rho) \quad \text{for} \quad \delta < \rho < 1 \qquad (26)$$

$$\sum_{m=0}^\infty a_m \frac{\rho^s \Gamma(1 + m + s)}{2\Gamma(2 + m)\Gamma(1 + s)} \,{}_2F_1(1 + m + s, -1 - m, 1 + s, \rho^2)$$

$$+ \sum_{l=0}^\infty b_l \frac{\rho^s \Gamma(1 + l + s)}{2\delta^s \Gamma(2 + l)\Gamma(1 + s)} \,{}_2F_1\left(1 + l + s, -1 - l, 1 + s, \frac{\rho^2}{\delta^2}\right) = 0 \quad \text{for} \quad 0 < \rho < \delta \qquad (27)$$

$$\rho = \frac{r}{a}, \quad \eta = a\xi, \quad \delta = \frac{b}{a}, \quad A(\eta) = \eta^2 B(\eta),$$

$$F_{sn}(\rho) = a^3 W_{sn}(\rho) \qquad (19)$$

Hence, the integral Eqs. (17) and (18) can be cast into the following form of the integral equations

$$\int_0^\infty A(\eta) J_s(\eta\rho) d\eta = -F_{sn}(\rho) \quad \delta < \rho < 1 \qquad (20)$$

$$\int_0^\infty \eta^{-1} A(\eta) J_s(\eta\rho) d\eta = 0 \quad \rho < \delta, \rho > 1 \qquad (21)$$

If the integral Eqs. (20) and (21) are solved for $A(\eta)$, then $B(\eta)$ can be derived using Eq. (19) and $\phi(r, z)$ using the inversion formula (16).

In this paper, we propose the use of Fourier-Bessel series for the above integral equation based on the approach used by Tranton (1950, 1954). In deriving the solution, we will use the following property of Bessel functions [Gradshteyn and Ryzhik, 1994; Eq. (5.574)].

$$\int_0^\infty x^{-1} J_{s+2n+2}(\alpha x) J_s(\beta x) dx = 0 \quad \text{for}$$

$$\beta > \alpha \quad \text{and} \quad n \geq 0 \qquad (22)$$

Hence, if we express $A(\eta)$ in terms of the following Bessel series,

$$A(\eta) = \sum_{m=0}^\infty a_m J_{s+2m+2}(\eta) + \sum_{l=0}^\infty b_l J_{s+2l+2}(\delta\eta) \qquad (23)$$

then Eq. (21) is automatically satisfied for $\rho > 1$. Inserting Eq. (23) into Eqs. (20) and (21), we obtain

where ${}_2F_1(a, b; c, x)$ represent the Hypergeometric function. Let us premultiply Eq. (27) by $\rho \,{}_2F_1(1 + q + s, -1 - q, 1 + s, (\rho^2/\delta^2))$ and integrate it from 0 to δ, and premultiplying Eq. (26) by $\rho \,{}_2F_1(\frac{3}{2} + p + s, -\frac{1}{2} - p, 1 + s, \rho^2)$ and integrate from δ to 1. Hence, we obtain

$$\sum_{m=0}^\infty a_m H_{pm} + \sum_{l=0}^\infty b_l H_{pl} = g_p \quad p = 0, 1, 2, \ldots \qquad (28)$$

$$\sum_{m=0}^\infty a_m H_{qm} + \sum_{l=0}^\infty b_l H_{ql} = 0 \quad q = 0, 1, 2, \ldots \qquad (29)$$

where

$$H_{pm} = \frac{\Gamma(\frac{3}{2} + m + s)}{\Gamma(\frac{3}{2} + m)\Gamma(1 + s)} \int_\delta^1 \rho^{s+1} \,{}_2F_1(\frac{3}{2} + p + s, -\frac{1}{2}$$

$$- p, 1 + s, \rho^2) \,{}_2F_1(\frac{3}{2} + m + s, -\frac{1}{2} - m, 1 + s, \rho^2) d\rho$$

$$\qquad (30)$$

$$H_{pl} = \frac{\delta^{2+2l+s}\Gamma(\frac{3}{2} + l + s)}{\Gamma(-\frac{1}{2} - l)\Gamma(3 + 2l + s)} \int_\delta^1 \rho^{-(2+2l+s)} \,{}_2F_1(\frac{3}{2} + p$$

$$+ s, -\frac{1}{2} - p, 1 + s, \rho^2) \,{}_2F_1\left(\frac{3}{2} + l + s, \frac{3}{2} + l,\right.$$

$$\left. 3 + 2l + s, \frac{\delta^2}{\rho^2}\right) d\rho \qquad (31)$$

$$H_{qm} = \frac{\Gamma(1 + m + s)}{2\Gamma(2 + m)\Gamma(1 + s)} \int_0^\delta \rho^{s+1} {}_2F_1\left(1 + q + s, -1 - q,\right.$$

$$\left. 1 + s, \frac{\rho^2}{\delta^2}\right) {}_2F_1(1 + m + s, -1 - m, 1 + s, \rho^2)d\rho \quad (32)$$

$$H_{ql} = \frac{\Gamma(1 + l + s)}{2\delta^s\Gamma(2 + l)\Gamma(1 + s)} \int_0^\delta \rho^{s+1} {}_2F_1\left(1 + q + s,\right.$$

$$\left. -1 - q, 1 + s, \frac{\rho^2}{\delta^2}\right) {}_2F_1\left(1 + l + s,\right.$$

$$\left. -1 - l, 1 + s, \frac{\rho^2}{\delta^2}\right)d\rho \quad (33)$$

$$g_p = \int_\delta^1 \rho F_{sn}(\rho) {}_2F_1\left(\tfrac{3}{2} + p + s, -\tfrac{1}{2}\right.$$

$$\left. - p, 1 + s, \rho^2\right)d\rho \quad (34)$$

Let us compute the velocity potential at the water-plate interface, which can be written as

$$\frac{\phi(\rho, 0)}{a} = \int_0^\infty \eta^{-1}A(\eta)J_s(\rho\eta)d\eta \quad \text{for} \quad \delta < \rho < 1 \quad (35)$$

Inserting Eq. (23) into Eq. (35) and using the mathematical table (Gradshteyn and Ryzhik, 1994), we can obtain

$$\frac{\phi(\rho, 0)}{a} = \sum_{m=0}^\infty \frac{a_m^*\rho^s\Gamma(1 + m + s)}{2\Gamma(2 + m)\Gamma(1 + s)} {}_2F_1\left(1 + m + s,\right.$$

$$\left. -1 - m, 1 + s, \rho^2\right), \quad \delta < \rho < 1 \quad (36)$$

where $a_m^* = -a_m/a^3$. Note that Eq. (36) is only valid for $\delta < \rho < 1$. The potential for $\rho > 1$ can be obtained but it is not necessary for the computation of the kinetic energy thus it is omitted.

The reference kinetic energy of the water can be written as

$$T_w^* = -\frac{1}{2}\rho_w \int_0^{2\pi} \int_0^\infty \frac{\partial\phi(r, 0)}{\partial z}\phi(r, 0)rdr\cos^2 s\theta d\theta$$

$$= -\frac{1}{2}\rho_w a^2 D_\theta \int_\delta^1 W_{sn}(\rho)\phi(\rho, 0)\rho d\rho \quad (37)$$

where

$$D_\theta = \begin{cases} 2\pi & \text{for} \quad s = 0, \\ \pi & \text{for} \quad s > 0. \end{cases} \quad (38)$$

Inserting Eq. (36) into Eq. (37), we obtain

$$T_w^* = \frac{1}{2}\rho_w a^3 D_\theta \sum_{m=0}^\infty \frac{a_m\Gamma(1 + m + s)}{2\Gamma(2 + m)\Gamma(1 + s)} \int_\delta^1 \rho^{s+1}W_{sn}(\rho){}_2F_1$$

$$\times (1 + m + s, -1 - m, 1 + s, \rho^2)d\rho \quad (39)$$

Note that T_w^* is the reference kinetic energy of water loaded on one side of the circular plate. If the circular plate is loaded on both sides therefore fully immersed in an unbounded fluid, the expression should be multiplied by 2.

The reference kinetic energy of the plate can be written as

$$T_p^* = \frac{1}{2}\rho_p h a^2 D_\theta \int_\delta^1 W_{sn}^2\rho d\rho \quad (40)$$

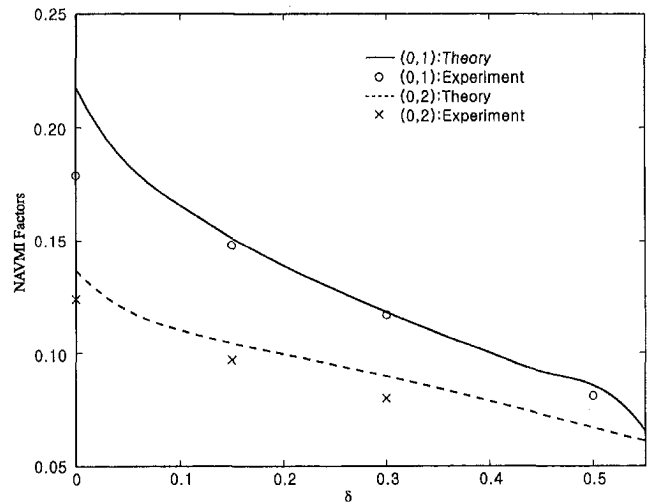If we choose coefficients which satisfy $\int_\delta^1 W_{sn}^2\rho d\rho = 1$, then

Fig. 1 NAVMI factors versus δ; $(s, n) = (0, 1)$, $(0, 2)$; s = number of nodal diameters; n = number of nodal circles

the nondimensionalized added virtual mass incremental factor, Γ_{sn}, based on Eq. (3) can be expressed as

$$\Gamma_{sn} = \sum_{m=0}^\infty \frac{a_m\Gamma(1 + m + s)}{2\Gamma(2 + m)\Gamma(1 + s)} \int_\delta^1 \rho^{s+1}W_{sn}(\rho){}_2F_1(1 + m$$

$$+ s, -1 - m, 1 + s, \rho^2)d\rho \quad (41)$$

Unfortunately, the integral appeared in Eq. (41) does not render a closed-form expression. Thus, we will resort to the numerical integration technique for the evaluation of this integral.

All the numerical computation including the integral appeared in Eq. (41) is carried out using Mathematica (Wolfram, 1988). It is found that up to $s = 5$ and $n = 5$, 10 term series expansion was enough for the evaluation of $A(\eta)$ as the coefficients for higher-order terms quickly converges to zero. The theoretical NAVMI factors, Γ_{sn}, for free-edge annular plates, for $(s, n) = (0, 1)$, $(0, 2)$, $(1, 1)$, $(2, 1)$, $(2, 0)$, $(3, 0)$ are shown as either solid or dashed lines in Figs. 1, 2 and 3.

3 Experiments and Discussion

The modal properties of three annular plates were experimentally determined, both in air (a condition which is very close to vacuum) and fully immersed in water. The annular plates are
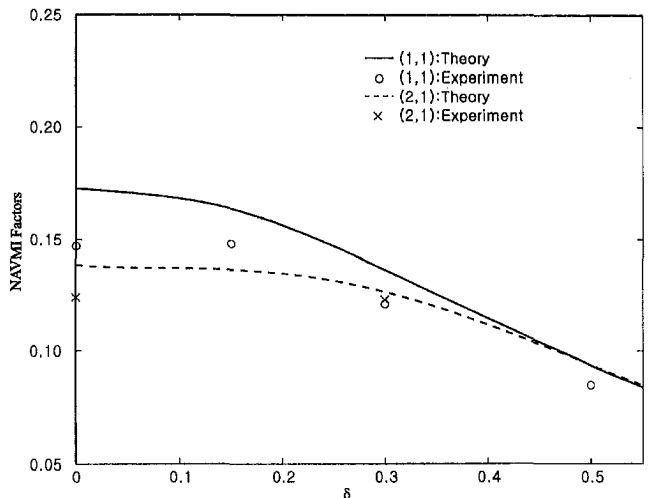

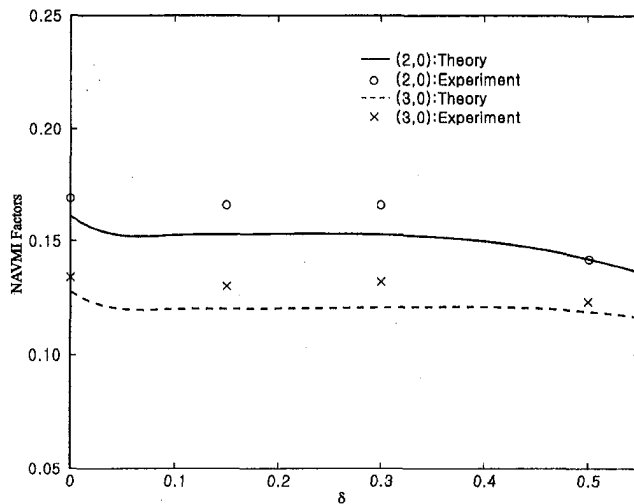Fig. 2 NAVMI factors versus δ; $(s, n) = (1, 1)$, $(2, 1)$

Fig. 3 NAVMI factors versus δ; $(s, n) = (2, 0), (3, 0)$

Fig. 4 Frequency Response Function (FRF) and its coherence for the annular plate with $\delta = 0.3$ immersed in water

manufactured by accurate laser cutting in order to prevent any deformation and using UNI Fe P 11 MG low carbon steel, according to the Italian standards. The Young's modulus is 206 GPa, the mass density is 7800 kg/m^3 and the Poisson ratio is $\nu = 0.3$, respectively. The thickness of the plates is 1.5 mm, the outer radius 100 mm for all plates and the inner radius 15, 30 and 50 mm, respectively. Thus, δ considered in the experiments are 0.15, 0.3, and 0.5.

All tests were carried out in a cylindrical tank with vertical axis having a diameter of 500 mm, which was built by gluing a Plexiglas transparent plate to a PVC pipe. The free-edge condition was obtained placing the test plates on a compliant suspension made by flexible wires. The plates were immersed in water 80 mm below the free surface. The total level of water in the tank was 180 mm. The plates were excited using a B & K (Brüel & Kjær) electro-dynamic exciter, model 4809, developing a maximum force of 45 N. The extremity of its stinger was glued to a point of the specimen, which is away from the center in order to excite the symmetric modes as well as asymmetric modes. The force was measured by a PCB 208A03 transducer and the response was measured by either a single-beam laser Doppler vibrometer Polytec OFV 1102 or an automatic scanning laser Doppler vibrometer Polytec PSV-100. Both sets can detect velocity up to 0.25 m/s. The noncontact vibration measurement techniques used in this experiment have a definite advantage over the measurement using an accelerometer since they do not add weight to a specimen. Furthermore, the weight of the accelerometer has an adverse effect on modes which may interfere the fluid-structure interaction; it changes the shape of the fluid-structure interface at the accelerometer location. The laser beam hits the plate through the transparent bottom of the tank and the water. In spite of such interfaces, the signal to noise ratio was confirmed affirmative by a good coherence as shown in Fig. 4. Figure 4 shows the frequency response function (FRF) and its coherence for the immersed annular plate with $\delta = 0.3$. A diagram of the experimental set-up is given in Fig. 5.

The modal analysis was carried out on the annular plate with $\delta = 0.3$ in air and the same plate immersed in water to check the assumption that wet mode shapes are almost identical with dry mode shapes. FRF's were measured at 48 different points and 16 of them were measured around each of three circumferences. Two circumferences were located very close to the edges (inner and outer); the last circumference was placed at an average radius with respect to the other two. The excitation was located at one of the 16 measured points of the last circle. The range of the measured FRF is from 0 Hz to 3200 Hz with a
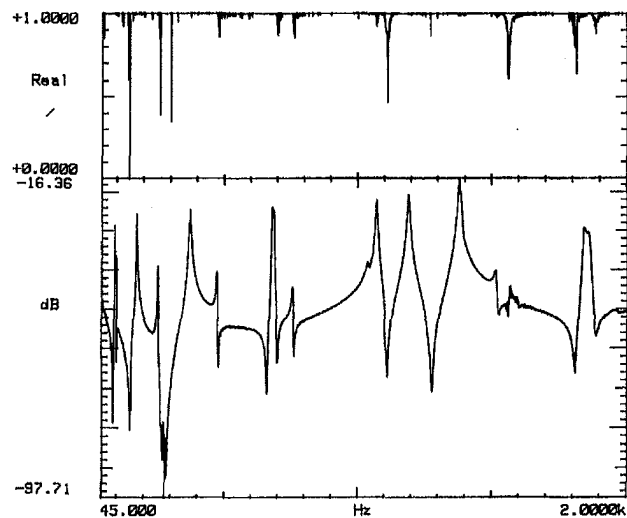
frequency resolution of 0.98 Hz. The sensor used is the single-beam laser Doppler vibrometer Polytec OFV 1102. The measurement of the FRF and the modal parameter estimation were performed by means of a HP 9000 workstation with DIFA Scadas II acquisition front-end and LMS CADA-X software for data acquisition and analysis. The FRF's were measured using 8 averages and estimated with the Hv method. The modal parameters were evaluated using the frequency domain direct parameter estimation method (Sas, 1993). The excitation signal was burst random with 50 percent of the signal in the sample period. Figure 6 shows the first three experimentally detected dry and wet mode shapes of the plate. In particular, the fundamental mode ($s = 2$, $n = 0$) presents split frequencies for the two coupled modes having the same shape but rotated by $\pi/2n$. This phenomenon is attributed to a loss of axisymmetry due to small defects of the specimen. As shown in the Fig. 6, the wet mode shapes are very close to the dry mode shapes, which validates the assumption introduced in the problem formulation.

Natural frequencies and mode shapes of the other two plates with inner radius of 15 and 50 mm were obtained using the automatic scanning laser Doppler vibrometer (SLV) Polytec PSV-100. The two plates were excited, in air and in water, by
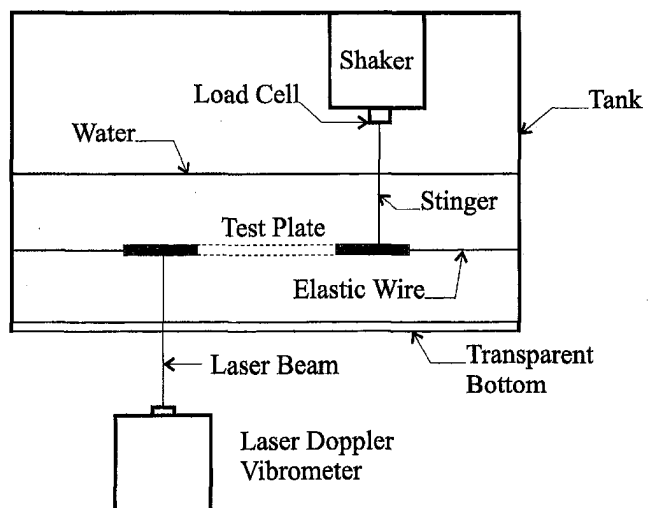

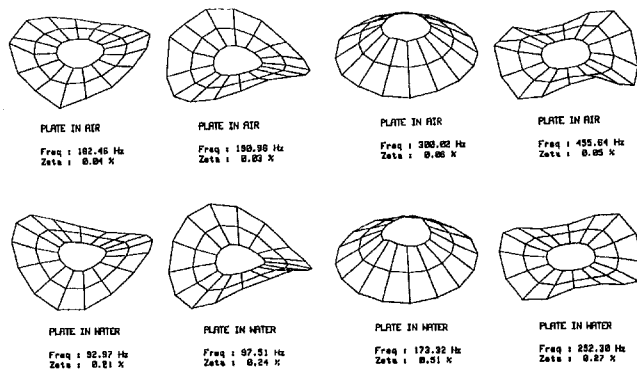**Fig. 5 Diagram of the experimental set-up**

Fig. 6 "Dry" and "Wet" mode shapes of the plate with $\delta = 0.3$ immersed in water

Table 1 Comparison of theoretical frequencies and experimental results for the plate with inner radius of 30 mm in air. Experimental damping factors of vibration in air are also given.

s	n	Theoretical (Hz)	Experimental (Hz)	Error (%)	Exp. Damping (%)
2	0	182.18	182.5	0.15	0.040
2	0	182.18	191.0	4.82	0.030
0	1	310.40	300.0	-3.34	0.055
3	0	455.16	455.6	0.11	0.051
3	0	455.16	464.8	2.12	0.077
1	1	680.92	651.0	-4.40	0.022
2	1	1226.86	1198.0	-2.36	0.020
0	2	1870.98	1833.0	-2.03	0.132
1	2	2183.80	2127.0	-2.60	0.025

a shaker using a burst random signal in order to estimate natural frequencies. Then, a fixed frequency sine wave excitation at the resonance frequency along with the SLV was used to obtain the mode shapes. Mode shapes are detected with good accuracy using this automatic scanning sensor, due to the large number of points that is possible to measure in a short period of time. Figure 7 shows the immersed mode shape of the annular plate which has an inner radius of 50 mm for the case of four nodal diameters and no nodal circle, i.e., $s = 4$, $n = 0$. A contour plot is used for the presentation of the mode shape. In this figure, the response is given as velocity and the contour plot is superimposed to a picture of the experimental apparatus (the shaker is located on the top-left part of the picture).

Natural frequencies detected experimentally in air on the three different plates are in good agreement with theoretical data presented by Vogel and Skinner (1965) and by Amabili et al. (1996). In Table 1, experimental natural frequencies are compared to computed frequencies for the plate having $\delta = 0.3$. The maximum error is less than 5 percent. Two different behaviors are observed for modes having no nodal circles ($n = 0$) and modes having nodal circles ($n > 0$); in the first case two coupled modes (identical mode shape but rotated by $\pi/2n$) were detected, and one of these has an excellent agreement with theoretical data, while the other has a little higher frequency. On the contrary, all modes with $n > 0$ show frequencies little lower than theoretical ones. In Table 1, experimentally detected damping factors are also shown; they are about 0.05 percent for listed modes. Damping factors range from 0.21 to 0.5 percent for the same plate completely immersed in water (Table 2); therefore a general increment of damping is observed in water. However, this damping is not high.

After measuring the natural frequencies in air and in water and identifying the corresponding modes, the NAVMI factors
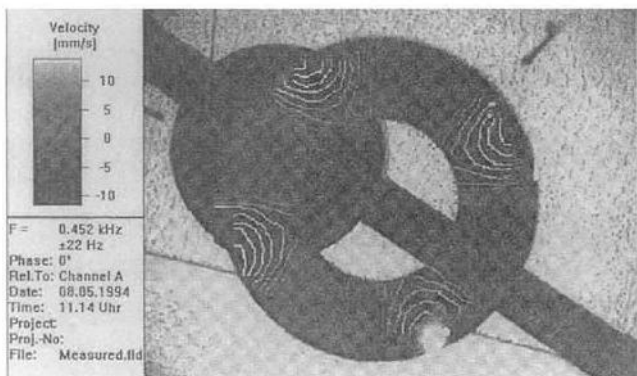
were evaluated based on Eqs. (2) and (3). Since the plates were immersed into water, the NAVMI factors were divided by 2 to represent the case of the plate resting on free surface. Those values are plotted as either a circle or a cross in Figs. 1, 2 and 3. As shown in those figures, the theoretical NAVMI factors agree quite well with the experimental results. Experimental data for $\delta = 0$ (circular plate) are taken from Amabili et al. (1995). It is shown that the natural frequencies in water computed by using the NAVMI factors are within 5 percent error. The error involved in the NAVMI factors is amplified because they appear in square root in the frequency relationship.

In the case of split experimental frequencies for the same mode, the average value of the NAVMI factor is presented in the figures. However, differences between these factors computed from the two couples of corresponding modes are small.

It is important to note that two main differences can be detected between the theoretical model and the performed experiments. First, the test tank has a finite radius and the water depth below the test plates is finite. Therefore the kinetic energy of water should be little increased in experiments with respect to the theoretical one, so that experimental NAVMI factors should be higher than those expected. Moreover, the distance between the test plate and the water free surface is finite (80 mm). Therefore free surface waves of the liquid are obtained as a consequence of the plate's vibration. This effect should reduce the measured NAVMI factors with respect to the actual ones. This effect was investigated by Amabili (1996) and shows a significant effect on some modes, especially for $\delta = 0$. These two differences give opposite effects on NAVMI factors. Therefore different errors between theoretical and experimental results are expected for different modes and values of δ. In particular, experimental NAVMI factors of modes (axisymmetric) given in Fig. 1 are below the theoretical values. A similar phenomenon is obtained for modes given in Fig. 2 (modes with one nodal circle). The opposite effect is shown by modes reported in Fig. 3 (modes without nodal circles). Hence, it seems that for our experiments the effect of finite fluid depth above the plate is larger for modes with nodal circles; in contrast, for modes without modal circles ($n = 0$), the finite tank dimension is more important.

An interesting phenomenon is that NAVMI factors decrease with δ for axisymmetric modes (Fig. 1) and modes with one nodal circle (Fig. 2), while they remain nearly the same for all the considered values of δ for modes without nodal circles (Fig.

Fig. 7 Mode shape for $s = 4$ and $n = 0$ of the annular plate with $\delta = 0.5$ immersed in water; natural frequency 448.2 Hz

Table 2 Comparison of theoretical frequencies and experimental results for the plate with inner radius of 30 mm immersed in water. Experimental damping factors of vibration in water are also given.

s	n	Theoretical (Hz)	Experimental (Hz)	Error (%)	Exp. Damping (%)
2	0	94.27	92.97	-1.40	0.22
2	0	94.27	97.51	3.32	0.24
0	1	180.76	173.3	-4.30	0.51
3	0	255.61	252.3	-1.31	0.27
1	1	377.33	371.1	-1.68	0.39
1	1	377.33	375.8	-0.41	0.36
2	1	688.97	678.7	-1.51	0.27
2	1	688.97	686.3	-0.39	0.21

3). Therefore it is possible to say that the effect of the dimension of the central hole on the fluid-structure interaction is small for modes without nodal circles and is large for axisymmetric modes. This is due to the fact that for modes with nodal circles and no nodal diameters, the parameter, δ is very important. In fact, for small δ values, there is a large relative movement between inner and outer plate's edge. On the contrary, this movement is small when δ becomes close to one. Therefore, the NAVMI factor decreases rapidly with δ as shown in Fig. 1. For modes without nodal circles, the influence of δ is small because the deflection in the central plate's area is small. Therefore, NAVMI factors remain almost constant for those modes, as shown in Fig. 3. For modes having both nodal circles and nodal diameters, there is a combined result, as shown in Fig. 2.

As a consequence of Eqs. (2) and (3), experimental NAVMI factors are evaluated with an increased error with respect to the error involved in the experimental natural frequencies of the immersed plates. The theoretical and experimental natural frequencies of the immersed plate with $\delta = 0.3$ are satisfactorily compared in Table 2.

4 Conclusions

Water has a significant effect on the vibration characteristics of structures in contact with water. In general, natural frequencies in water are smaller than those in air because the total kinetic energy increases due to the presence of water. This phenomena is often explained in terms of virtual mass increase. Assuming that the wet mode shapes are the same as the ones in air, we are able to separate the coupled problem into independent boundary value problems. Then, the change of natural frequency subjected to certain mode shape due to the presence of water can be predicted by the Rayleigh quotient, which depends on the added virtual mass incremental (AVMI) factor.

In this paper, the nondimensionalized added virtual mass incremental (NAVMI) factors are obtained for the uniform annular plates resting on free surface. To verify the theoretical results, experiments were carried out and it is found that the experimental results agree well with the theoretical results. It is generally found that the NAVMI factor decreases as number of nodal diameter and nodal circles increases, which has the same tendency as observed in the circular plates. It is also found that the NAVMI factors decrease as the ratio of inner and outer radii increases.

Acknowledgments

References

1 Amabili, M., 1994, "Modal Properties of Annular Plates Vibrating in Water," *Proceedings of the First International Conference on Vibration Measurements by Laser Techniques: Advances and Applications,* Ancona, Italy, October 3–5, pp. 421–429.

2 Amabili, M., 1996, "Effect of Finite Fluid Depth on the Hydroelastic Vibrations of Circular and Annular Plates," *Journal of Sound and Vibration,* Vol. 193, No. 4, pp. 909–925.

3 Amabili, M., Dalpiaz, G., and Santolini, C., 1995, "Free-Edge Circular Plates Vibrating in Water," *Modal Analysis: The International Journal of Analytical and Experimental Modal Analysis,* Vol. 10, No. 3, pp. 187–202.

4 Amabili, M., Frosali, G., and Kwak, M. K., 1996, "Free Vibration of Annular Plates Coupled with Fluids," *Journal of Sound and Vibration,* Vol. 191, pp. 825–846.

5 Espinosa, F. M., and Gallego-Juarez, J. A., 1984, "On the Resonance Frequencies of Water-Loaded Circular Plates," *Journal of Sound and Vibration,* Vol. 94, No. 2, pp. 217–222.

6 Gradshteyn, I. S., and Ryzhik, I. M., 1994, *Table of Integrals, Series and Products, 5th Edition,* Academic Press, London.

7 Kwak, M. K., 1991, "Vibration of Circular Plates in Contact with Water," ASME *Journal of Applied Mechanics,* Vol. 58, pp. 480–483.

8 Kwak, M. K., 1994, "Vibration of Circular Membranes in Contact with Fluid," *Journal of Sound and Vibration,* Vol. 178, No. 5, pp. 688–690.

9 Kwak, M. K., 1997, "Hydroelastic Vibration of Circular Plates," *Journal of Sound and Vibration,* Vol. 201, No. 3, pp. 293–303.

10 Kwak, M. K., and Kim, K. C., 1991, "Axisymmetric Vibration of Circular Plates in Contact with Fluid," *Journal of Sound and Vibration,* Vol. 146, No. 3, pp. 381–389.

11 Lamb, H., 1921, "On the Vibrations of an Elastic Plate in contact with Water," *Proceedings of the Royal Society of London, Series A,* Vol. 98, pp. 205–216.

12 McLachlan, N. W., 1932, "The Accession to inertia of Flexible Discs Vibrating in a Fluid," *Proceedings of the Physical Society (London),* Vol. 44, pp. 546–555.

13 Meirovitch, L., 1986, *Elements of Vibration Analysis,* 2nd ed., McGraw-Hill Book Company, New York.

14 Peake, W. H., and Thurston, E. G., 1954, "The Lowest Resonant Frequency of a Water-Loaded Circular Plate," *Journal of the Acoustical Society of America,* Vol. 26, No. 7, pp. 166–168.

15 Powell, J. H., and Roberts, J. H. T., 1923, "On the Frequency of Vibration of Circular Diaphragms," *Proceedings of the Physical Society (London),* Vol. 35, pp. 170–182.

16 Lord Rayleigh, 1945, *Theory of Sound* (two volumes), second edition, Dover Publications, New York.

17 Sas, P., ed., 1993, *Course on Modal Analysis Theory and Practice* (2 volumes), *Proceedings of the 18th International Seminar on Modal Analysis,* Katholieke Universiteit, Leuven, Belgium.

18 Sneddon, I. N., 1951, *Fourier Transforms,* McGraw-Hill, New York.

19 Tranton, C. J., 1950, "On Some Dual Integral Equations Occurring in Potential Problems with Axial Symmetry," *Quarterly Journal of Mechanics and Applied Mathematics,* Vol. 3, No. 4, pp. 411–419.

20 Tranton, C. J., 1954, "A Further Note on Dual Integral Equations and an Application to the Diffraction of Electromagnetic Waves," *Quarterly Journal of Mechanics and Applied Mathematics,* Vol. 7, No. 3, pp. 317–325.

21 Vogel, S. M., and Skinner, D. W., 1965, "Natural Frequencies of Transversely Vibrating Uniform Annular Plates," ASME *Journal of Applied Mechanics,* Vol. 32, pp. 926–931.

22 Wolfram, S., 1988, *Mathematica: A System of Doing Mathematics by Computer,* Addison-Wesley, Redwood City, CA.